STEM CELLS

Sphingosine kinases protect murine embryonic stem cells from sphingosine-induced cell cycle arrest

Suveg Pandey[1] | Kelly M. Banks[1] | Ritu Kumar[1] | Andrew Kuo[2,3] | Duancheng Wen[4] | Timothy Hla[2,3] | Todd Evans[1] (ORCID)

[1]Department of Surgery, Weill Cornell Medicine, New York, New York

[2]Vascular Biology Program, Boston Children's Hospital, Boston, Massachusetts

[3]Department of Surgery, Harvard Medical School, Boston, Massachusetts

[4]Center for Reproductive Medicine, Weill Cornell Medicine, New York, New York

Correspondence
Todd Evans, PhD, Department of Surgery, Weill Cornell Medicine, 1300 York Ave., LC-704, New York, NY.
Email: tre2003@med.cornell.edu

Abstract

Sphingosine-1-phosphate (S1P) is a bioactive lipid molecule regulating organogenesis, angiogenesis, cell proliferation, and apoptosis. S1P is generated by sphingosine kinases (SPHK1 and SPHK2) through the phosphorylation of ceramide-derived sphingosine. Phenotypes caused by manipulating S1P metabolic enzymes and receptors suggested several possible functions for S1P in embryonic stem cells (ESCs), yet the mechanisms by which S1P and related sphingolipids act in ESCs are controversial. We designed a rigorous test to evaluate the requirement of S1P in murine ESCs by knocking out both *Sphk1* and *Sphk2* to create cells incapable of generating S1P. To accomplish this, we created lines mutant for *Sphk2* and conditionally mutant (floxed) for *Sphk1*, allowing evaluation of ESCs that transition to double-null state. The *Sphk1/2*-null ESCs lack S1P and accumulate the precursor sphingosine. The double-mutant cells fail to grow due to a marked cell cycle arrest at G2/M. Mutant cells activate expression of telomere elongation factor genes *Zscan4*, *Tcstv1*, and *Tcstv3* and display longer telomeric repeats. Adding exogenous S1P to the medium had no impact, but the cell cycle arrest is partially alleviated by the expression of a ceramide synthase 2, which converts excess sphingosine into ceramide. The results indicate that sphingosine kinase activity is essential in mouse ESCs for limiting the accumulation of sphingosine that otherwise drives cell cycle arrest.

1 | INTRODUCTION

Sphingosine-1-phosphate (S1P) is a bioactive lipid molecule of the lysophospholipid family that can promote cell migration, proliferation, and survival. The role of S1P as a key signaling molecule regulating development, homeostasis, and disease is well established, with many biological effects mediated through a family of five specific G-protein-coupled receptors termed S1P receptors 1-5 (S1PR1-5).[1] Although best studied for a role in regulating vascular integrity and lymphocyte trafficking, it has also been reported that S1P signaling mediates proliferation of embryonic stem cells (ESCs), neural stem cells, and cancer stem cells.[2-9] S1P is generated through phosphorylation of sphingosine, carried out by the sphingosine kinases. The relative abundance of sphingosine and S1P is balanced by sphingosine kinases and phosphatases.[1,10]

There are two genes encoding sphingosine kinases, sphingosine kinase 1 (*Sphk1*) and sphingosine kinase 2 (*Sphk2*). The two proteins are well conserved across vertebrate evolution and share a high degree of sequence similarity, with the larger ortholog SPHK2 comprising almost all the entirety of SPHK1, but with a 36 amino acid addition at the N-terminus and a proline-rich polypeptide insert in the central region.[11] The

cellular localization of the two enzymes varies, with SPHK1 found mainly in the cytoplasm. SPHK1 activation, mediated by phosphorylation of the Serine 225 residue by the extracellular signal-regulated kinase 1/2 (ERK1/2),[12] relocates the protein to the plasma membrane where it converts sphingosine to S1P. In contrast, SPHK2 has the capacity to enter the nucleus, owing to a nuclear localization signal, and can be modulated when phosphorylated by protein kinase D (PKD).[13] However, SPHK2 can also be found in the endoplasmic reticulum in response to serum deprivation.[14] Over-expression studies indicate that at least in some contexts, the two proteins may have opposing functions in regulating ceramide biosynthesis[14] and proliferation.[15,16] Yet despite these differences, studies with knockout mice indicate that they have at least some redundant functions during embryonic development. Specifically, mice with knockout of either *Sphk1*[17] or *Sphk2*[18] are viable and fertile and neither single knockout causes any obvious developmental defects. In contrast, mice lacking both *Sphk1* and *Sphk2* die in utero due to severe defects in neurogenesis and angiogenesis.[18] Double mutant embryos at E12.5 have cell loss in the forebrain, increased apoptotic cells in the neuroepithelium of the telencephalon and diencephalon, and decreased mitotic cells in the telencephalon.

Compared with somatic cells, ESCs have a very short G1 phase and undergo cell division much more rapidly than somatic cells.[19] In fact, rapid proliferation is thought to be required for the maintenance of ESC identity,[20] and cells undergoing differentiation elongate their G1 phase[21] while cells undergoing induced pluripotency contract their G1 phase.[22] The impact of S1P has been studied using both mouse ESCs (mESCs) and human ESCs (hESCs), as recently reviewed.[23] In mESCs, addition of S1P stimulates proliferation through activation of STAT3[24] and ERK[3,25] pathways, dependent on S1PRs. S1P stimulation of S1PR1 and S1PR3 was reported to transactivate FLK1 leading to enhanced mESC proliferation.[3] Raising S1P levels by dysregulating sphingosine lyase enhanced expression of mESC core pluripotency genes.[24] Exogenous S1P can also stimulate hESC proliferation, through ERK, p38, and c-Jun N-terminal Kinase (JNK) signaling, and in cooperation with platelet-derived growth factor suppresses apoptosis.[4] However, in the hESC model, exogenous S1P was reported to downregulate significantly pluripotency gene expression levels.[8] Since the pluripotent state of the two cell types is different, with hESCs at a "primed" compared with the murine "naïve" stage, results may need to be interpreted in this context. However, in general, the existing literature suggests that S1P signaling is primarily pro-proliferative. Notably, most studies have relied on addition of exogenous S1P or forced expression of sphingosine kinase to investigate its role, which can be complicated by receptor presentation, metabolism by lyases and phosphatases, and feedback mechanisms. A rigorous test of the de novo synthesis pathway in ESCs has not been characterized previously. We designed a strategy to generate sphingosine kinase null ESCs and report a critical role for sphingosine kinase activity in maintaining mESC proliferation.

Significance statement

The function of the sphingosine-1-phosphate (S1P) signaling pathway in embryonic stem cells (ESCs) has been unclear. A genetic approach was used to eliminate S1P from murine ESCs by deleting both sphingosine kinase orthologs. It was found that loss of both kinases is incompatible with ESC proliferation, as the cells arrest at the G2/M checkpoint. However, the defect is not caused by lack of S1P but rather from accumulation of sphingosine, because the phenotype can be reverted by expression of ceramide synthase. The data are consistent with previous results from early zebrafish embryos, suggesting a key conserved role for limiting sphingosine levels in stem and progenitor cells.

2 | MATERIALS AND METHODS

2.1 | Generation of mESC lines

Sphk1^{fl/fl}; *Sphk2*^{−/−} female mice were superovulated with pregnant mare serum gonadotropin (PMSG) (G4877, Sigma, St. Louis, MO) and human chorionic gonadotropin (hCG) (CG10, Sigma). Each female received 5 IU PMSG through intraperitoneal injection (i.p.) 48 hours following injection of 5 IU hCG (i.p.). Females were mated with *Sphk1*^{fl/fl}; *Sphk2*^{−/−} males. The two-cell stage embryos were flushed from the oviducts and cultured in EmbryoMax KSOM medium (MR-107-D, Millipore, Burlington, MA) to obtain blastocysts. A 96-well plate was prepared and seeded with mouse embryonic fibroblasts (MEFs) in Dulbecco's modified Eagle's medium (DMEM) supplemented with 10% fetal bovine serum (FBS) overnight, and then changed to an ESC deriving medium (EDF1) (KnockOut DMEM [GIBCO, Dublin, Ireland] with 20% KnockOut Serum Replacement [GIBCO], 1% penicillin-streptomycin [Millipore], 1% L-glutamine [Millipore], 1% nonessential amino acids (Millipore), 1% 100× EmbryoMAX Nucleosides [Millipore], 1% EmbryoMAX beta-mercaptoethanol [Millipore], 0.25% PD98059 [Promega, Madison, WI], 0.02% recombinant mouse LIF [Chemicon, Temecula, CA]) prior to plating of embryos. Zonae pellucidae of the blastocysts were removed with brief exposure to Tyrode's saline solution, after which denuded embryos were washed 3× in 30 μL of EDF1 medium, and placed individually into a well. After 4-5 days, the inner cell mass (ICM) outgrowths from the blastocysts emerged and the cell clumps were dissociated with 20 μL of 0.025% trypsin for 5-10 minutes, resuspended with 200 μL of EDF1 medium, and transferred to new wells with feeders for further culture for 2-3 days until emergence of ESC colonies. ESC colonies were further expanded in EDF1 medium for 2-3 passages and switched to normal ESC medium after the ESC lines were established. In some experiments, the wildtype R1 line was used as control.

2.2 | Cell culture

mESCs were grown in a medium of KnockOut DMEM (ThermoFisher, Waltham, MA) with 1% GlutaMAX Supplement (ThermoFisher), 1% penicillin-streptomycin (GIBCO), 1% modified Eagle's medium (MEM) nonessential amino acids solution (GIBCO), 0.1 mM 2-mercaptoethanol (GIBCO), 10^3 units/mL ESGRO Recombinant Mouse LIF Protein (Millipore), and 15% FBS (Sigma). Cells were cultured on irradiated

C57BL/6 MEFs (GIBCO) at a density of 2×10^6 cells/10-cm dish. Cells were counted using a Cellometer Vision cytometer (Nexcelom, Lawrence, MA) as per manufacturer's instructions. To induce Cre-mediated excision of the *Sphk1* gene, (Z)-4-hydroxytamoxifen (Sigma) was added at a concentration of 6 μM for 48 hours. For S1P addback experiments, S1P was sonicated in albumin and added to medium at 1 μM.

2.3 | Sphingosine kinase activity assay

Frozen mESC pellets (feeder free, approximately 10^7 cells each sample) were resuspended in sphingosine kinase (SK) activity buffer (20 mM Tris pH 7.4, 150 mM NaCl, 1 mM ethylenediamine tetraacetic acid (EDTA), 15 mM NaF, 15 mM NaF, 40 mM β-glycerophosphate, and proteinase inhibitors cocktail [Sigma]) and lysed by three short bursts of 10-second sonications with 30 seconds of cooling between bursts. Cell homogenates were centrifuged at 720*g* at 4°C for 5 minutes to remove nuclear fraction followed by 10 000*g* at 4°C for 5 minutes to remove mitochondrial fraction. Protein concentration of the remaining supernatant containing cytosolic and membrane fractions was determined by the Bio-Rad Dc Protein Assay. SK activity reaction was initiated by supplementing 50-200 μg of protein lysates with a final concentration of 10 μM C17-sphingosine (Avanti, Alabaster, Alabama), 500 μM ATP, with/without 10 μM sphingosine kinase inhibitor (SKI, Cayman, Ann Arbor, Michigan) in SK activity buffer. The reactions were incubated at 37°C for 0, 30, or 60 minutes and stopped by freezing the reaction in liquid nitrogen. Lipids were extracted and C17-S1P synthesized in the reactions was measured by the Lipidomics Shared Core at Stony Brook Cancer Center.

2.4 | Immunostaining

Immunostaining was performed by fixing mESCs in Millicell glass EZ slide (Millipore) with 4% paraformaldehyde (Sigma) at room temperature (RT) for 20 minutes. Cells were blocked for an hour by incubating in phosphate-buffered saline (PBS) supplemented with 10% FBS, 0.1% IgG-free bovine serum albumin (BSA, Jackson ImmunoResearch, West Grove, Pennsylvania) and 0.1% saponin from quillaja bark (Sigma) at RT. Cells were incubated overnight at 4°C with anti-SPHK1 (Abcam, Cambridge, UK, 1:50) or anti-SPHK2 antibody (Abcam, 1:50) in blocking buffer. Fluorescence-conjugated secondary antibody was used for visualization. Nuclei were labeled with 4′,6-diamidino-2-phenylindole (Molecular Probes, Invitrogen, Carlsbad, California). Images were collected on a Zeiss (Oberkochen, Germany) LSM 800 confocal microscope with ZEN software. To measure NANOG, the same protocol was used except that mESCs were fixed in a tissue culture dish, stained with anti-NANOG antibody (Abcam, 1:100) and visualized on a Zeiss epifluorescence microscope with the AxioVision software.

2.5 | Microscopy and flow cytometry analysis

Cells were kept in PBS and 1% Bovine Albumin Fraction (GIBCO) for the duration of fluorescent analysis. Fluorescent images were taken using a Zeiss Axio Observer.Z1 microscope and captured using a Zeiss AxioCam CCD camera. For flow, cells were dissociated with Accutase (StemCell Technologies, Vancouver, Canada) at 37°C for 5 minutes and collected in DMEM + 15% FBS media. Cells were centrifuged and resuspended in PBS with 1% Bovine Albumin Fraction (GIBCO). Flow cytometry was conducted using either Attune NxT (ThermoFisher) or Accuri C6 (BD Biosciences, Bedford, Massachusetts) analyzers consistent with manufacturer's instructions.

2.6 | Adenovirus and lentiviral production

The adenoviral expression vectors Ad5-CMV-GFP and Ad5-CMV-Cre-GFP were purchased from the Baylor College of Medicine Vector Development Lab. Two lentiviral destination expression vectors were designed and purchased from VectorBuilder Inc (Chicago, Illinois). One vector uses the EF1A promoter to drive expression of Cre-ERT2, followed by a P2A self-cleaving peptide and then Turbo-GFP. A second vector uses the EF1A promoter to drive expression of human ceramide synthase 2 (CERS2) fused to a flexible linker peptide (3xGGGS) followed by mRFP1. To generate viruses, HEK-293T cells were plated at 70% confluence in 10-cm dishes, and for each dish, 3 μg VSVG, 2.5 μg REV, 5 μg RRE, and 15 μg lentiviral destination expression plasmids were combined, then added to a premixed media with 44.8 μL of polyethylenimine in 1.5 mL of DMEM (VWR, Radnor, Pennsylvania), with an additional 7 mL of DMEM for 5 hours. Media was then replaced with DMEM with 15% FBS, 1% penicillin-streptomycin, and 1% GlutaMAX for 48 hours, then collected, centrifuged at 3000 rpm for 15 minutes. The remaining supernatant was filtered through a 0.45-μm polyurethane membrane, mixed with 1:3 volumes of Lenti-X Concentrator (Clontech/Takara, Mountain View, California), and left overnight at 4°C. After centrifugation at 1500*g* for 45 minutes, the pellet was resuspended in cell culture media.

2.7 | Quantitative reverse transcription-polymerase chain reaction (qRT-PCR)

Equal numbers of cells were sorted using FACS Aria (BD) or Influx (BD) from the Weill Cornell Flow Cytometry or Leukemia Biorespository Core Facilities using green fluorescent protein (GFP) and red fluorescent protein (RFP) gates. Total RNA was extracted using the RNeasy Kit (Qiagen, Hilden, Germany), and cDNA was generated with 1 μg total RNA using SuperScript VILO cDNA Synthesis Kit (ThermoFisher). LightCycler 480 SYBR Green 1 Master Mix (Roche, Basel, Switzerland) was used to analyze cDNA by quantitative RT-PCR using the Light Cycler 480II (Roche). Cycle conditions for the reactions were 95°C for 15 minutes, followed by 40 cycles of 94°C for 14 seconds, 55°C for 30 seconds, and 72°C for 30 seconds. Ct values were calculated using the ΔΔCt method based on the median value from a triplicate set.[26] To measure telomeres, DNA was extracted from sorted cells using DNeasy Kit (Qiagen). Twenty nanograms of DNA were used to measure relative telomere length using primers 36B4 and parameters as previously described.[27]

2.8 | Cell cycle analysis

Equal numbers of cells were sorted using FACS Aria (BD) or Influx (BD) from the Weill Cornell Flow Cytometry or Leukemia Biorepository Core Facilities using GFP and RFP gates. Cells were fixed in 500 μL of 70% EtOH overnight at −20°C. Fixed cells were washed and resuspended in FxCycle PI/RNase Staining Solution (ThermoFisher) at a concentration of 1 million cells/1 mL solution and incubated at RT away from light for 20 minutes before analysis via flow cytometry as described above.

2.9 | Lipidomic analysis

Equal numbers of cells were sorted using FACS Aria (BD) or Influx (BD) from the Weill Cornell Flow Cytometry or Leukemia Biorepository Core Facilities using GFP and RFP gates. Cells were pelleted and submitted to the analytical core facility at the Medical University of South Carolina for ceramide and sphingolipid analysis. Sphingolipids were extracted after the addition of internal standards and quantified by liquid chromatography with tandem mass spectrometry as described previously.[28]

2.10 | Quantitative fluorescent in situ hybridization and karyotyping

Cells for quantitative fluorescent in situ hybridization (QFISH) of telomeres were cultured, induced, and sorted as described above. Two hours before dissociation for FACS sorting, cells were treated with 50 μL/mL Colcemid (Invitrogen), and submitted postsort to the Molecular Cytogenetics Core at the Memorial Sloan Kettering Cancer Center. Cells for karyotyping were cultured as described above and submitted directly to the Molecular Cytogenetics core.

2.11 | RNA sequencing

Equal numbers of cells were sorted using FACS Aria (BD) or Influx (BD) from the Weill Cornell Flow Cytometry or Leukemia Biorepository Core Facilities using GFP and RFP gates. Total RNA was extracted using the RNeasy Kit (Qiagen). Samples were submitted for quality control, and samples exceeding RNA integrity number >7 were selected for cDNA library preparation. Library preparation and sequencing was conducted by the Genomics Resources Core Facility at Weill Cornell Medicine using a HiSeq4000 next-generation sequencer (Illumina, San Diego, California). Differential expression was analyzed in R with the DeSeq2 package. Heatmaps with hierarchical clustering were generated in R using the CRAN package for a subset of the most differentially expressed genes. Following normalization of the RNA Sequencing counts in DeSeq, z scores were computed across samples within each gene for use in the heatmaps.

2.12 | Primers

For genotyping via PCR:

Spk1loxF: GGA CCT GGC TAT GGA ACC (common forward primer).

Spk1loxR1: ATG TTT CTT TCG AGT GAC CC (250 bp flox band).

Spk1loxR2: AAT GCC TAC TGC TTA CAA TAC C (600 bp KO band).

For qPCR:

ZScan4 F: GAGATTCATGGAGAGTCTGACTGATGAGTG.

ZScan4 R: GCTGTTGTTTCAAAAGCTTGATGACTTC.

Tcstv1 F: TGAACCCTGATGCCTGCTAAGACT.

Tcstv1 R: AGATGGCTGCAAAGACACAACTGC.

Tcstv3 F: AGAAAGGGCTGGAACTTGTGACCT.

Tcstv3 R: AAAGCTCTTTGAAGCCATGCCCAG.

Gapdh F: CCCCAATGTGTCCGTCGTG.

Gapdh R: GCCTGCTTCACCACCTTCT.

Telomere F: CGGTTTGTTTGG GTTTGGGTTTGGGTTTGGGTTT GGGTT.

Telomere R: GGCTTGCCTTACCCTTACCCTTACCCTTACCCTT ACCCT.

36B4 F: ACTGGTCTAGGACCCGAGAAG.

36B4 R: TCAATGGTGCCTCTGGAGATT.

3 | RESULTS

3.1 | Derivation of conditional sphingosine kinase null ESC lines

A previously characterized *Sphk2* knockout strain was bred to mice carrying a floxed *Sphk1* allele to generate *Sphk1*^{fl/fl}; *Sphk2*^{−/−} mice, which are viable and fertile.[18,29-31] These mice were inbred, developing blastocysts were isolated, and cells of the ICM plated to generate individual mESC clones. Individual clones were expanded and validated as pluripotent based on colony morphology and expression of NANOG (Figure 1A). Multiple individual clones were confirmed by genotyping and shown to have normal karyotypes (Figure 1B). Although representative results are usually shown for one clone, all experiments were repeated with two independent clones (4 and 10) throughout this study, and the results were fully consistent with both clones.

3.2 | Sphingosine kinase null stem cell colonies fail to grow

Mass spectrometry was used to show that mESCs have active sphingosine kinase activity, based on the accumulation of S1P upon addition to cellular lysates of exogenous sphingosine, which was blocked in the presence of the sphingosine kinase inhibitor compound SKI (Supporting Information Figure S1A). We next verified that SPHK1 and SPHK2 are both expressed in mESCs. Immunofluoresence assays using specific antibodies confirmed, as indicated above from studies
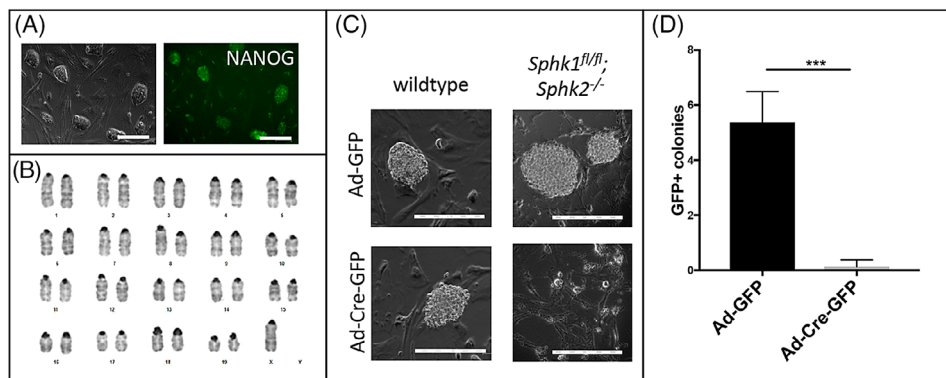
FIGURE 1 *Sphk$^{fl/fl}$; Sphk2$^{-/-}$* ESCs transduced with an adenovirus expressing Cre recombinase shows that ESCs lacking sphingosine kinase are impaired at colony formation. A, Representative mESC colonies from a line derived from *Sphk1$^{fl/fl}$; Sphk2$^{-/-}$* blastocysts. Left panel shows characteristic mESC colony morphology (cultured on top of MEF feeder cells), right panel shows immunofluorescent staining for the expression of pluripotency marker NANOG. White bars are 100 μ. B, Representative example of a *Sphk1$^{fl/fl}$; Sphk2$^{-/-}$* mESC karyotype showing a grossly normal genome. C, Wildtype mESCs form colonies with an equivalent efficiency when transduced with adenovirus expressing either GFP alone, or a Cre-GFP fusion protein (left panels). In contrast, *Sphk1$^{fl/fl}$; Sphk2$^{-/-}$* mESCs form colonies with the GFP-expressing vector, but rarely form colonies when transduced with the Cre-GFP vector (right panels). White bars indicate 50 μm. D, Quantification of relative colony forming capacity from four independent experiments shows a significant difference in colony forming potential between GFP-expressing (Ad-GFP) and Cre-expressing (Ad-Cre-GFP) cells. Data are derived by counting colonies across random fields of view at 20× magnification, which were averaged for each independent experiment. Data are presented as SE of the mean, analyzed by Student's *t* test, ***$P < .001$. See also Supporting Information Figure S1. ESCs, embryonic stem cells; GFP, green fluorescent protein; MEF, mouse embryonic fibroblast; mESC, mouse embryonic stem cell

in other contexts, that in mESCs SPHK1 is primarily cytoplasmic or at the plasma membrane, while SPHK2 is primarily nuclear (Supporting Information Figure S1B). In an initial set of experiments, we attempted to knockout the *Sphk1* gene through transduction of an adenoviral vector that coexpresses the Cre recombinase with a GFP reporter, which should in principle generate sphingosine kinase null cells. Using wildtype cells, GFP+ colonies were isolated following transduction with vectors that express either GFP alone or Cre and GFP. GFP+ colonies were also recovered when the *Sphk1$^{fl/fl}$; Sphk2$^{-/-}$* ESCs were transduced with a vector expressing only GFP. However, we recovered few if any colonies when these cells coexpressed Cre (Figure 1C, D), precluding their analysis.

Therefore, to evaluate the consequence of sphingosine kinase loss, a conditional system was generated using a lentiviral vector encoding a *CreERT2-P2A-TurboGFP* cassette. Following transduction, cells were allowed to form colonies for 24 hours after plating, and then treated with vehicle as control, or induced with tamoxifen to activate CreERT2. In this case, cells induced with tamoxifen were found to exhibit a striking difference in growth. Both colony size and colony number were reduced 48 hours after induction, with the GFP (Cre) expressing cells notably diminished (Figure 2A). The result was confirmed by flow cytometry, which demonstrated that the GFP-positive population was depleted upon induction of Cre with tamoxifen (Figure 2B). The reduction in cell growth observed for *Sphk1$^{fl/fl}$; Sphk2$^{-/-}$* ESCs was not seen using wildtype ESCs that were infected and treated under the same conditions (Figure 2C), indicating the phenotype is dependent on the conditional loss of *Sphk1* on the *Sphk2* null background. The results suggest that complete loss of sphingosine kinase activity is incompatible with ESC growth.

3.3 | Sphingosine kinase knockout leads to sphingosine and ceramide accumulation

To examine how the growth phenotype correlates with lipid biology, lipidomic profiles were examined before and after induction of Cre activity. Under both conditions, S1P levels in cell lysates were below detectable thresholds, under 0.1 pmol/mL (Figure 3A). This suggests that at baseline, mESCs do not maintain a high intracellular level of S1P. This is consistent with results from Brimble et al,[32] who measured sphingolipid intermediates in hESCs, which were found to have much lower S1P levels compared to MEFs. However, the sphingosine levels in lysates from cells induced for Cre activity to knockout sphingosine kinase activity were significantly higher than in lysates from uninduced cells (Figure 3B). Similarly, the levels of the upstream precursor ceramide were also elevated in the induced cells (Figure 3C). The lipidomic profiling showed a broad range increase in all ceramide and sphingosine species (Supporting Information Figure S2). Therefore, sphingosine kinases are normally active in mESCs to phosphorylate sphingosine, presumably to generate S1P that is either turned over or exported.

3.4 | Cells lacking sphingosine kinase display a G2/M cell cycle arrest

Because the GFP-expressing (Cre-induced) population was specifically depleted from cells in culture, cells were selected for GFP expression using flow cytometry, in order to directly compare the GFP+ cells with the control GFP− population from the same transduction. In this case,
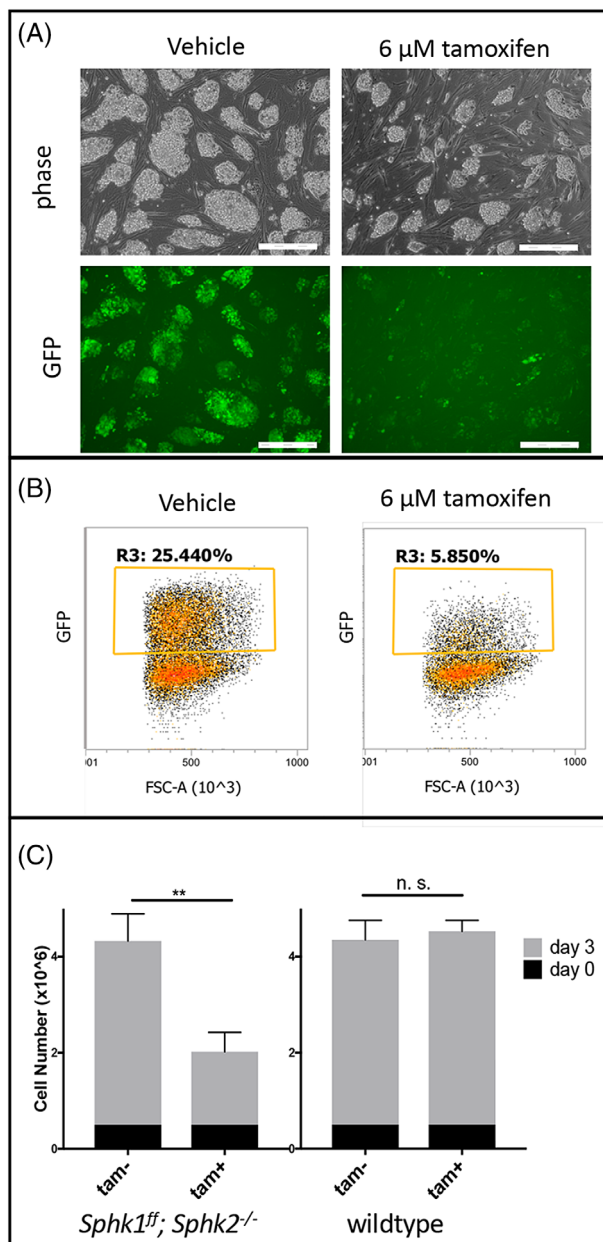
FIGURE 2   Induction of Cre enzyme to generate sphingosine kinase null mESCs creates a diminished capacity to grow. A, In a representative experiment, *Sphk1^{fl/fl}; Sphk2^{−/−}* cells were transduced with a lentiviral vector expressing GFP and CreERT2 and the replated cells subsequently treated either with DMSO, vehicle) or tamoxifen (right panels). Upon induction of Cre recombinase activity, cells formed fewer, smaller colonies (shown in top panels by phase microscopy) and those that do form are comprised almost entirely of GFP− (and thus Cre−) cells. White bars indicate 100 μm. B, Representative flow cytometry assay also showing the relative depletion of GFP-expressing cells in the populations induced for Cre expression by tamoxifen. C, Cumulative data from three independent experiments shows (left panel) *Sphk1^{fl/fl}; Sphk2^{−/−}* cultures that were initiated (day 0) with equal cell numbers and treated with vehicle (tam−) or 6 μM tamoxifen (tam+) for 3 days display a significant difference in growth. Wildtype cells treated in the same manner (right panel) do not show differential growth, indicating the effect is specific to the loss of sphingosine kinase activity. Data are presented as SE of the mean, analyzed by Student's *t* test, ***P < .001. DMSO, dimethylsulfoxide; mESCs, mouse embryonic stem cells; n.s., not significant

the GFP− cells will retain the *Sphk1* gene, while the floxed alleles will be excised in the Cre/GFP+ population. Propidium iodide (PI) staining was used to measure the relative distribution of cells in different phases of the cell cycle. Cells in the GFP− control compartment (Cre −) display a distribution characteristic of normally dividing cells, with the highest peak corresponding to cells in the G0/G1 phase, and a second peak at double the PI signal, indicating cells in the G2/M phase (Figure 4A). Kinase null cells in the Cre/GFP+ compartment display a significantly perturbed distribution, with a much enhanced G2/M peak, indicating that a large number of cells fail to exit out of the G2/M checkpoint. This experiment was carried out three times using wildtype ESCs, in which case the cell cycle profiles in GFP− and Cre/GFP+ cells were unchanged (Figure 4B), indicating that the arrest seen in the Cre/GFP+ compartment of cells with floxed *Sphk1* alleles is not due to lentiviral infection or expression of GFP or Cre, but is specific to the loss of *Sphk1*. Two independent *Sphk1^{fl/fl}; Sphk2^{−/−}* clones were used to profile GFP+ and GFP− compartments by RNA sequencing. The gene set enrichment analysis showed that the most enriched gene set in the GFP+ compartment conformed to a hallmark G2/M checkpoint (Figure 4C), consistent with the cell-cycle analysis.

3.5 | Loss of sphingosine kinase stimulates expression of telomere lengthening proteins

In addition to the G2/M checkpoint profile, two families of genes most prominently upregulated in the GFP+ cells were *Zscan4* and *Tcstv1/3* (Figure 5A). These transcripts were confirmed to be highly increased in GFP+ cells in subsequent independent experiments by qRT-PCR (Figure 5B). These genes have been shown to function in mESCs for elongating telomeres.[33,34] We note that expression levels for canonical telomere length regulation, *Tert* and *Terc*, were not affected (Figure 5C). To confirm the functional effect of this program, telomeric repeat lengths were compared in the DNA of sorted GFP+ and GFP− cells using quantitative PCR. On average, telomere repeats were twofold to fourfold more abundant in the GFP+ compartment, depending on the clone (Figure 5D). Although less quantitative, telomeres were also evaluated for length by fluorescence in situ hybridization. The chromosome spreads derived from the GFP+ samples contained a number of chromosomes with particularly high levels of fluorescence (Figure 5E), suggesting that the increased telomere repeat lengths are chromosome selective rather than a general phenomenon.

3.6 | Overexpression of ceramide synthase can partially rescue loss of sphingosine kinase

The phenotypes described above could be caused by the inability of mutant cells to generate S1P. However, addition of 1 μM S1P to the medium was unable to rescue colony-forming capacity of Cre-induced mutant cells. Based on our previous studies in the zebrafish embryo,[28] we hypothesized that cell cycle arrest might instead be due to
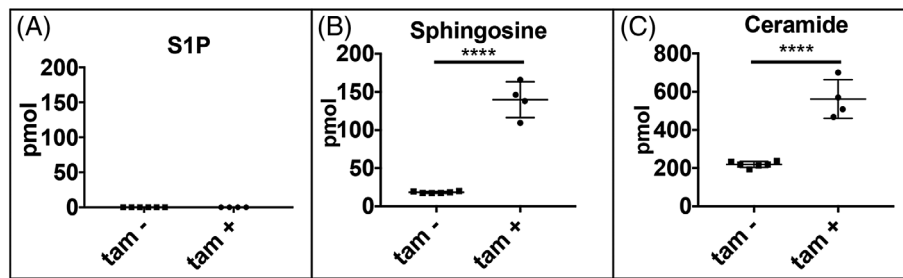
FIGURE 3 Lipidomic profiling shows that sphingosine kinase knockout causes accumulation of sphingosine and ceramide. *Sphk1*$^{fl/fl}$; *Sphk2*$^{-/-}$ cells were transduced with a lentiviral vector expressing CreERT2 and the cells treated either for 48 hours with DMSO (tam−) or tamoxifen (tam+). Measured by quantitative mass spectrometry, in either case the cellular lysates had undetectable levels of S1P (A) but those induced for Cre activity showed accumulated levels of sphingosine (B) and ceramide (C) compared to uninduced cells. Levels are indicated as pmol per sample. Each sample was derived from a six-well plate seeded with 250 K cells, but lipids were also normalized to cell number at the time of processing. Data were derived from six (tam−) or four (tam+) independent experiments. Data are presented as SE of the mean, analyzed by Student's *t* test, ****$P < .0001$. See also Supporting Information Figure S2. S1P, Sphingosine-1-phosphate; DMSO, dimethylsulfoxide
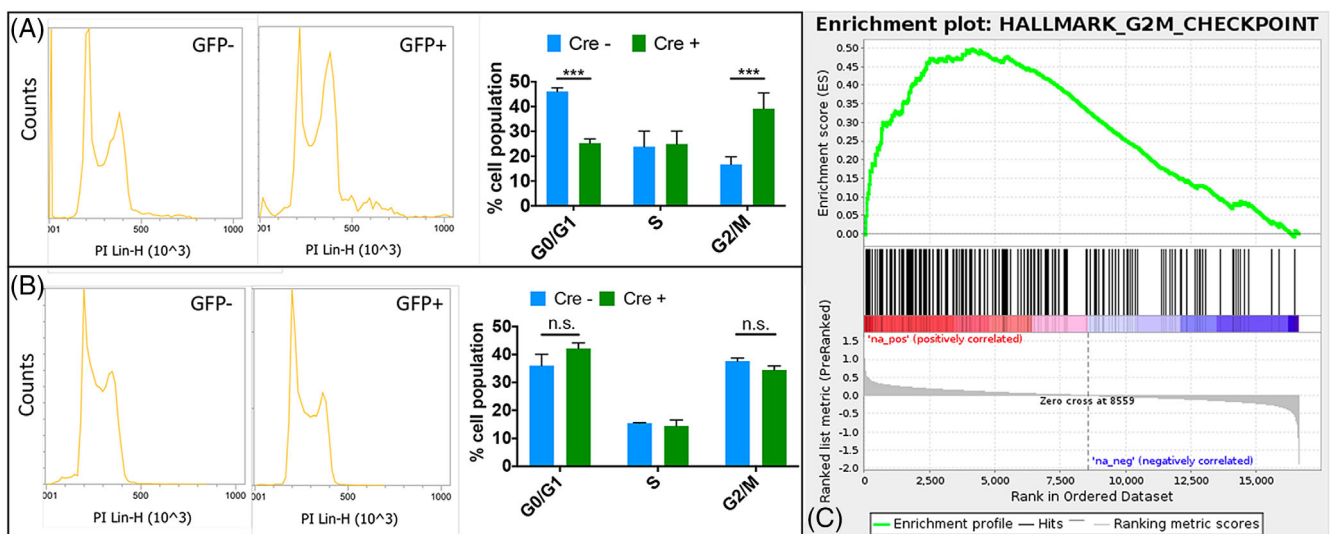

FIGURE 4 Analysis of cell cycle by flow cytometry shows that sphingosine kinase null cells display a cell cycle defect with arrest at G2/M. A, *Sphk1*$^{fl/fl}$; *Sphk2*$^{-/-}$ cells were transduced with a lentiviral vector coexpressing CreERT2 and GFP, and following induction with tamoxifen, cells were sorted according to GFP expression to separate cells with and without expression of Cre recombinase. Sorted cells were assayed with propidium iodide for DNA content, in order to evaluate cell cycle stages. As shown in a representative flow analysis, the (GFP+) Cre-expressing compartment displayed a relatively increased proportion of the cell population in G2/M. Cumulative results from three independent experiments are shown on the right. Data are presented as SE of the mean, analyzed by Student's *t* test, ***$P < .001$. B, When wildtype mESCs were treated under identical conditions, the cell cycle profiles in Cre-expressing and nonexpressing cell populations did not differ. C, Two independent mESC lines were treated in the same manner in two independent experiments (four GFP− and four GFP+ biological replicates each) and profiled for differential transcript expression by RNA sequencing. According to Gene Set Enrichment Analysis the hallmark G2/M checkpoint transcriptional program was the most differentially expressed geneset. GFP, green fluorescent protein; mESCs, mouse embryonic stem cells; n.s., not significant

excessive accumulation of sphingosine in the mutant ESCs. Multiple *Cers* genes are expressed in mESCs, especially *Cers2* and *Cers5* (Supporting Information Figure S3). However, unlike zebrafish embryos, the kinase mutant mESCs do not upregulate any of the *Cers* gene family members. Therefore, we sought to alleviate sphingosine accumulation by forced expression of CERS2 (for this purpose we chose human CERS2). *Sphk1*$^{fl/fl}$; *Sphk2*$^{-/-}$ cells were transduced, in addition to a lentiviral vector encoding *CreERT2-P2A-TurboGFP*, with a lentiviral vector containing an *Ef1a-CERS2-RFP* expression construct.

The CERS2-RFP is a fusion protein that allows purification of CERS2-expressing cells by FACS. Cells were coinfected with the two lentiviral expression vectors and sorted according to both Cre expression (GFP) and CERS2 expression (RFP). Cell populations were gated to isolate negative, single- or double-positive populations (gating and controls are shown in Supporting Information Figure S4) and evaluated for cell cycle profiles using PI. Forced expression of CERS2 alone did not affect cell cycle, while cells expressing Cre alone recapitulated the cell cycle arrest previously documented (Figure 6A). The double-
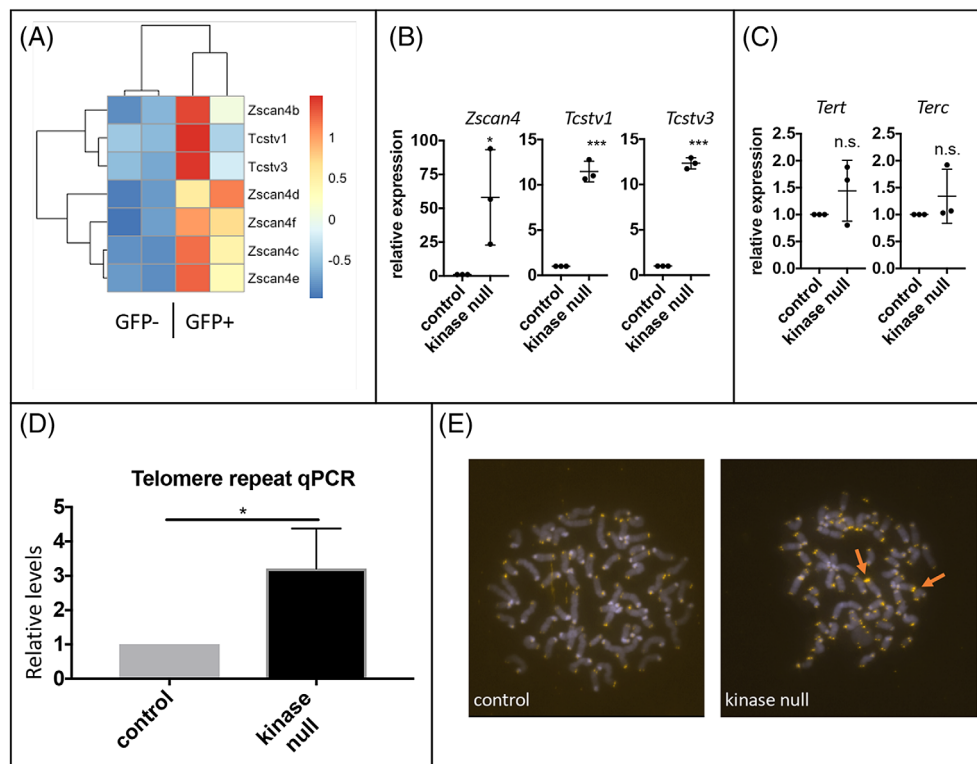
FIGURE 5 Transcript profiling and FISH analysis shows that loss of sphingosine kinase activates a telomere-elongation program. A, From the RNA-sequencing profiles, among the most differentially expressed genes were *Zscan4* and *Tcstv* family members. Heatmaps are based on two independent experiments using transduced cells that were GFP– (no Cre expression, left lanes) or GFP+ (Cre expressing, right lanes). B, Three independent experiments using sorted control (GFP–) and kinase null (GFP+) cells confirmed by qPCR that kinase null cells express significantly higher levels of transcripts for *Zscan4*, *Tcstv1*, and *Tcstv3*. Note that primers do not distinguish individual *Zscan4* orthologs. C, In contrast, transcripts of components of the telomerase holoenzyme including *Tert*, the reverse transcriptase, and *Terc*, the RNA component, were expressed at similar levels between control and kinase null cells. D, Based on qPCR, telomeric repeat regions in genomic DNA of GFP+ (kinase null) cells are significantly higher than those of GFP– (control) cells. E, Shown are representative individual mitotic spreads of control (GFP–) or kinase null (GFP+) cells probed by FISH for telomeres. The mutant cells display particularly bright signals on some but not all chromosomes (indicated by red arrows in the right panel). Data in B–D are presented as SE of the mean, analyzed by Student's *t* test, *$P < .05$, ***$P < .001$. FISH, fluorescent in situ hybridization; GFP, green fluorescent protein; PI, propidium iodide; RFP, red fluorescent protein; qPCR, quantitative polymerasechain reaction

positive population, comprising kinase null cells expressing CERS2-RFP, showed a partial rescue of the cell cycle arrest caused by Cre expression. Additionally, when these cells were sorted and plated in equal numbers, cells expressing CERS2-RFP alone could generate ESC colonies, while those expressing only Cre (GFP) were defective at forming colonies, as expected. Overexpression of CERS2-RFP in the kinase null cells largely restored their ability to form ESC colonies (Figure 6B). Lipidomic profiling showed that forced expression of CERS2-RFP in Cre-expressing cells lowered the amounts of cellular sphingosine and ceramide, validating the association of increased levels and cell cycle arrest (Figure 6C).

4 | DISCUSSION

The role of the S1P signaling pathway in regulating ESC biology has been unclear, but several reports suggested a positive influence on cell proliferation. Here we used a rigorous genetic strategy that clearly defines a requirement for regulating sphingosine metabolism in the context of cell cycle. Despite different cellular locations and signaling mechanisms reported for the two kinases, previous work suggested that the two sphingosine kinases serve redundant functions during early embryogenesis, in that either single knockout is tolerated, but the loss of both genes results in embryonic lethality around E11.5-E12.5 due to defects in neurogenesis and angiogenesis.[18] Initial attempts to target the two genes using CRISPR/Cas9 failed, presumably due to strong selective pressure for cells that retained a functional allele. Likewise, small molecule inhibitors were not informative, since compounds that are specific for SPHK2 are not available. Therefore, we chose to use a conditional knockout approach, using previously validated null alleles. We found that loss of both sphingosine kinases is not tolerated in mESCs, since we could not recover colonies in *Sphk1*$^{fl/fl}$; *Sphk2*$^{-/-}$ ESCs that were induced to activate a conditional Cre enzyme. Evaluation of the Cre-induced cells showed a specific block at the G2/M checkpoint, consistent with a cell proliferation defect. Since this phenotype was at least partially rescued by the forced expression of CERS2, it appears to be caused by accumulation of sphingosine, rather than a lack of S1P. This is entirely consistent
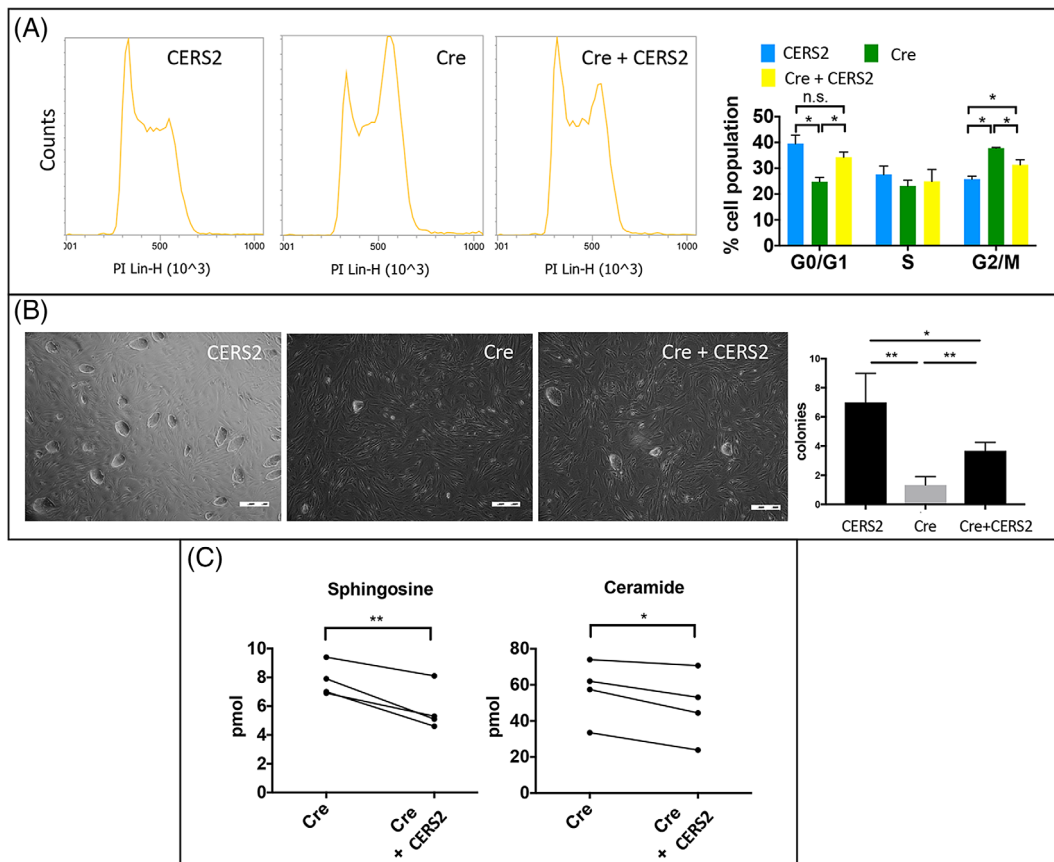
FIGURE 6 Flow cytometry and colony formation assays show that forced expression of ceramide synthase partially overcomes the loss of sphingosine kinases. Cells were transduced with two lentiviral vectors expressing Cre-GFP or CERS2-RFP and after tamoxifen induction, sorted based on the expression of CERS2 (RFP only), Cre (GFP only) or both Cre and CERS2 (RFP + GFP), and equal numbers of cells postsort were assayed for cell cycle profiles using propidium iodide and flow cytometry. A, Representative flow plots for PI, and on the right, cumulative results from three independent experiments. Forced expression of CERS2 in a kinase null background (yellow) showed a significant (albeit partial) rescue of the G2/M cell cycle arrest (green). B, Cells sorted as described above were plated in equal numbers and assayed for colony forming ability. Shown are representative fields, and (right panel), cumulative results from three independent experiments. White bars indicate 100 μ. C, Cells similarly treated were sorted for kinase null (Cre) and CERS2 rescue (Cre + CERS2) populations and assayed by lipidomics. From four independent experiments, overexpression of CERS2 lowered the amount of intracellular sphingosine (left) and ceramide (right). Data are presented as SE of the mean, analyzed by Student's t test, *P < .05, **P < .01. See also Supporting Information Figures S3 and S4

with our previous studies using the zebrafish model that discovered an early role for sphingosine kinases, likely even during oogenesis. In this case, embryos lacking sphingosine kinase manage to compensate by the upregulating expression of a single *cers* gene, *cers2b*, as a salvage pathway to reduce excess sphingosine, which otherwise causes embryonic demise during gastrulation.[35] Since the murine *Cers2* gene is not upregulated in ESCs to rescue the phenotype, we do not place any significance on CERS2 per se for the partial rescue shown in the ESC context by forced expression.

It may be that zebrafish embryos develop until gastrulation because early dividing blastomeres do not have normal somatic cell cycle checkpoints. With this compensation, although the zebrafish embryos are developmentally delayed, they survive until S1P is needed to control cardiac progenitor migration in a receptor-dependent process. It is unclear why the mESCs do not upregulate *Cers2* upon loss of sphingosine kinases, but we can speculate that this might happen during oogenesis or early development in double mutant mouse embryos,

which allows them to develop until S1P is presumably needed, around midgestation. Although previous genetic experiments[18] and our data in mESCs indicate redundant functions for *Sphk1* and *Sphk2* during mouse development, the different cellular locations and different biological outputs reported for the two kinases suggest that they likely have distinct nonredundant roles in the context of homeostasis and disease.

An important problem for cell proliferation during genome replication is the maintenance of telomeres.[36] The depletion of telomeric repeats with each cell division is a well-characterized problem that can lead to genomic instability, G1 cell cycle arrest, and senescence.[37,38] Notably, it has been shown that an accumulation of ceramide in adenocarcinoma cells depletes telomeres by way of destabilizing telomerase.[39] S1P, on the other hand, has been shown to bind to human telomerase reverse transcriptase and stabilize telomerase in lung cancer cells.[40] We found that mESCs lacking sphingosine kinase activity have elongated telomere repeats. However, the mechanism does not appear to be through telomerase. Instead, the arrested cells strikingly upregulate

transcripts for many variants of *Zscan4*, as well as the genes *Tcstv1* and *Tcstv3*. These genes have been shown in mESCs to work together to elongate telomeres specifically through the telomere sister chromatid exchange (T-SCE) mechanism, which is capable of extending telomere lengths in a rapid fashion.[33] T-SCE is an alternate mechanism to telomerase-mediated maintenance and is activated in mESCs when telomeres are critically shortened.[41] It is possible that the upregulation of *Zscan4*, *Tcstv1*, and *Tcstv3* and the elongation of telomeres are a downstream effect of the cell cycle arrest, as *Zscan4* has been shown to be differentially activated as a compensatory mechanism for cell cycle extension.[42] Concurrently, TCSTV1 and TCSTV3 have been suggested to stabilize ZSCAN4 in mESCs.[34] Given that *Tert* and *Terc* transcripts are not significantly upregulated in the sphingosine kinase null cells and that ceramide accumulation has been shown to rapidly deplete telomere lengths,[39] it is likely that T-SCE is the method used to restore telomere lengths in mESCs upon sphingosine kinase loss. Our results were obtained using murine ESCs, since we could take advantage of the validated genetic tools. However, given that mESCs and hESCs are in distinct states of pluripotency (naïve and primed, respectively), it is premature to assume the same requirements for sphingosine kinases in hESCs, pending further studies.

5 | CONCLUSIONS

Murine ESCs that lack sphingosine kinase activity arrest cell cycle at G2/M and activate the T-SCE mechanism to extend telomere lengths. The cell cycle arrest can be partially alleviated by the expression of *Cers2*, indicating that sphingosine kinase activity is essential in ESCs not for generating S1P, but rather for limiting the accumulation of sphingosine that otherwise drives cell cycle arrest.

CONFLICT OF INTEREST
T.H. declared patent applications filed from WCM and BCH, advisory role with Bridge Medicine, Sun Pharma Adv Res Co. (SPARC), research funding from ONO Pharmaceuticals and expert testimony for Steptoe & Johnson LLP. All of the other authors declared no potential conflicts of interests.

AUTHOR CONTRIBUTIONS
S.P.: performed experiments, analyzed data, and wrote the manuscript; K.B.: carried out data analysis and provided figures; R.K.: performed experiments and analyzed data; A.K.: performed experiments and analyzed data; D.W.: generated mESC lines and provided these key unpublished tools; T.H.: conceived and designed the study and provided key reagents and financial support; T.E.: conceived and designed the study, analyzed data, wrote the manuscript, and provided financial support.

DATA AVAILABILITY STATEMENT
Raw data from RNA sequencing experiments is available on the GEO public database, accession number: GSE139964.

ORCID
Todd Evans https://orcid.org/0000-0002-7148-9849

REFERENCES
1. Mendelson K, Evans T, Hla T. Sphingosine 1-phosphate signalling. *Development*. 2014;141(1):5-9.
2. Pebay A, Wong RC, Pitson SM, et al. Essential roles of sphingosine-1-phosphate and platelet-derived growth factor in the maintenance of human embryonic stem cells. *STEM CELLS*. 2005;23(10):1541-1548.
3. Ryu JM, Baek YB, Shin MS, et al. Sphingosine-1-phosphate-induced Flk-1 transactivation stimulates mouse embryonic stem cell proliferation through S1P1/S1P3-dependent beta-arrestin/c-Src pathways. *Stem Cell Res*. 2014;12(1):69-85.
4. Wong RC, Tellis I, Jamshidi P, Pera M, Pébay A. Anti-apoptotic effect of sphingosine-1-phosphate and platelet-derived growth factor in human embryonic stem cells. *Stem Cells Dev*. 2007;16(6):989-1001.
5. Hirata N, Yamada S, Shoda T, Kurihara M, Sekino Y, Kanda Y. Sphingosine-1-phosphate promotes expansion of cancer stem cells via S1PR3 by a ligand-independent Notch activation. *Nat Commun*. 2014;5:4806.
6. Shen H, Zhou E, Wei X, et al. High density lipoprotein promotes proliferation of adipose-derived stem cells via S1P1 receptor and Akt, ERK1/2 signal pathways. *Stem Cell Res Ther*. 2015;6:95.
7. Bieberich E. It's a lipid's world: bioactive lipid metabolism and signaling in neural stem cell differentiation. *Neurochem Res*. 2012;37(6):1208-1229.
8. Avery K, Avery S, Shepherd J, Heath PR, Moore H. Sphingosine-1-phosphate mediates transcriptional regulation of key targets associated with survival, proliferation, and pluripotency in human embryonic stem cells. *Stem Cells Dev*. 2008;17(6):1195-1205.
9. Callihan P, Alqinyah M, Hooks SB. Sphingosine-1-phosphate (S1P) signaling in neural progenitors. *Methods Mol Biol*. 2018;1697:141-151.
10. Olivera A, Allende ML, Proia RL. Shaping the landscape: metabolic regulation of S1P gradients. *Biochim Biophys Acta*. 2013;1831(1):193-202.
11. Pitson SM. Regulation of sphingosine kinase and sphingolipid signaling. *Trends Biochem Sci*. 2011;36(2):97-107.
12. Pitson SM, Moretti PA, Zebol JR, et al. Activation of sphingosine kinase 1 by ERK1/2-mediated phosphorylation. *EMBO J*. 2003;22(20):5491-5500.
13. Ding G, Sonoda H, Yu H, et al. Protein kinase D-mediated phosphorylation and nuclear export of sphingosine kinase 2. *J Biol Chem*. 2007;282(37):27493-27502.
14. Maceyka M, Sankala H, Hait NC, et al. SphK1 and SphK2, sphingosine kinase isoenzymes with opposing functions in sphingolipid metabolism. *J Biol Chem*. 2005;280(44):37118-37129.
15. Igarashi N, Okada T, Hayashi S, Fujita T, Jahangeer S, Nakamura SI. Sphingosine kinase 2 is a nuclear protein and inhibits DNA synthesis. *J Biol Chem*. 2003;278(47):46832-46839.
16. Liu H, Toman RE, Goparaju SK, et al. Sphingosine kinase type 2 is a putative BH3-only protein that induces apoptosis. *J Biol Chem*. 2003;278(41):40330-40336.
17. Allende ML, Sasaki T, Kawai H, et al. Mice deficient in sphingosine kinase 1 are rendered lymphopenic by FTY720. *J Biol Chem*. 2004;279(50):52487-52492.

18. Mizugishi K, Yamashita T, Olivera A, Miller GF, Spiegel S, Proia RL. Essential role for sphingosine kinases in neural and vascular development. *Mol Cell Biol*. 2005;25(24):11113-11121.

19. Becker KA, Ghule PN, Therrien JA, et al. Self-renewal of human embryonic stem cells is supported by a shortened G1 cell cycle phase. *J Cell Physiol*. 2006;209(3):883-893.

20. Ruiz S, Panopoulos AD, Herrerías A, et al. A high proliferation rate is required for cell reprogramming and maintenance of human embryonic stem cell identity. *Curr Biol*. 2011;21(1):45-52.

21. White J, Dalton S. Cell cycle control of embryonic stem cells. *Stem Cell Rev*. 2005;1(2):131-138.

22. Ghule PN, Medina R, Lengner CJ, et al. Reprogramming the pluripotent cell cycle: restoration of an abbreviated G1 phase in human induced pluripotent stem (iPS) cells. *J Cell Physiol*. 2011;226(5):1149-1156.

23. Lidgerwood GE, Pitson SM, Bonder C, Pébay A. Roles of lysophosphatidic acid and sphingosine-1-phosphate in stem cell biology. *Prog Lipid Res*. 2018;72:42-54.

24. Smith GS, Kumar A, Saba JD. Sphingosine phosphate lyase regulates murine embryonic stem cell proliferation and pluripotency through an S1P2/STAT3 signaling pathway. *Biomolecules*. 2013;3(3):351-368.

25. Rodgers A, Mormeneo D, Long JS, Delgado A, Pyne NJ, Pyne S. Sphingosine 1-phosphate regulation of extracellular signal-regulated kinase-1/2 in embryonic stem cells. *Stem Cells Dev*. 2009;18(9):1319-1330.

26. Livak KJ, Schmittgen TD. Analysis of relative gene expression data using real-time quantitative PCR and the 2(-delta delta C(T)) method. *Methods*. 2001;25(4):402-408.

27. Callicott RJ, Womack JE. Real-time PCR assay for measurement of mouse telomeres. *Comp Med*. 2006;56(1):17-22.

28. Mendelson K, Pandey S, Hisano Y, et al. The ceramide synthase 2b gene mediates genomic sensing and regulation of sphingosine levels during zebrafish embryogenesis. *Elife*. 2017;6:e21992.

29. Pappu R, Schwab SR, Cornelissen I, et al. Promotion of lymphocyte egress into blood and lymph by distinct sources of sphingosine-1-phosphate. *Science*. 2007;316(5822):295-298.

30. Xiong Y, Lee HJ, Mariko B, et al. Sphingosine kinases are not required for inflammatory responses in macrophages. *J Biol Chem*. 2016;291(21):11465.

31. Xiong Y, Yang P, Proia RL, Hla T. Erythrocyte-derived sphingosine 1-phosphate is essential for vascular development. *J Clin Invest*. 2014;124(11):4823-4828.

32. Brimble SN, Sherrer ES, Uhl EW, et al. The cell surface glycosphingolipids SSEA-3 and SSEA-4 are not essential for human ESC pluripotency. *Stem Cells*. 2007;25(1):54-62.

33. Zalzman M, Falco G, Sharova LV, et al. Zscan4 regulates telomere elongation and genomic stability in ES cells. *Nature*. 2010;464(7290):858-863.

34. Zhang Q, Dan J, Wang H, et al. Tcstv1 and Tcstv3 elongate telomeres of mouse ES cells. *Sci Rep*. 2016;6:19852.

35. Mendelson K, Lan Y, Hla T, Evans T. Maternal or zygotic sphingosine kinase is required to regulate zebrafish cardiogenesis. *Dev Dyn*. 2015;244(8):948-954.

36. Gunes C, Rudolph KL. The role of telomeres in stem cells and cancer. *Cell*. 2013;152(3):390-393.

37. Bodnar AG, Ouellette M, Frolkis M, et al. Extension of life-span by introduction of telomerase into normal human cells. *Science*. 1998;279(5349):349-352.

38. d'Adda di Fagagna F, Reaper PM, Clay-Farrace L, et al. A DNA damage checkpoint response in telomere-initiated senescence. *Nature*. 2003;426(6963):194-198.

39. Sundararaj KP, Wood RE, Ponnusamy S, et al. Rapid shortening of telomere length in response to ceramide involves the inhibition of telomere binding activity of nuclear glyceraldehyde-3-phosphate dehydrogenase. *J Biol Chem*. 2004;279(7):6152-6162.

40. Panneer Selvam S, de Palma RM, Oaks JJ, et al. Binding of the sphingolipid S1P to hTERT stabilizes telomerase at the nuclear periphery by allosterically mimicking protein phosphorylation. *Sci Signal*. 2015;8(381):ra58.

41. Wang Y, Erdmann N, Giannone RJ, Wu J, Gomez M, Liu Y. An increase in telomere sister chromatid exchange in murine embryonic stem cells possessing critically shortened telomeres. *Proc Natl Acad Sci USA*. 2005;102(29):10256-10260.

42. Nakai-Futatsugi Y, Niwa H. Zscan4 is activated after telomere shortening in mouse embryonic stem cells. *Stem Cell Reports*. 2016;6(4):483-495.

SUPPORTING INFORMATION

Additional supporting information may be found online in the Supporting Information section at the end of this article.